Mechanical and Energy Engineering

Heat Transfer Analysis of Conventional Round Tube and Microchannel Condensers in Automotive Air Conditioning System

Issam Mohammed Ali Aljubury*
Instructor
Mech. Eng. Dept.
College of Eng.- Univ. of Baghdad
drissam@uobaghdad.edu.iq

Muayad Abdulnabi Mohammed
Researcher
Mech. Eng. Dept.
College of Eng.- Univ. of Baghdad
Muayad.24@yahoo.com

ABSTRACT

In this paper, an experimental analysis of conventional air-cooled and microchannel condensers in automotive vapor compression refrigeration cycle concerning heat transfer coefficient and energy using R134a as a refrigerant was presented. The performance of two condensers and cycles tested regarding ambient temperature which it was varied from $40^{o}C$ to $65^{o}C$, while the indoor temperature and load have been set to be $23^{o}C$ and 2200 W respectively. Results showed that the microchannel condenser has 224 % and 77 % higher refrigerant side and air side heat transfer coefficient respectively than the coefficients of the conventional condenser. Thus, the COP, in case of using the microchannel condenser, was found to be 20 % higher than that of the conventional cycle. Also, the microchannel condenser has a 50 % smaller volume than the conventional. Therefore, it provides more space in the car engine container occupied with other components.

Keywords: Automotive air conditioning, Condenser, Microchannel, Heat transfer coefficient, Energy.

تحليل انتقال حرارة لمكثف تقليدي دائري الانبوب ومكثف مايكروي في نظام تكييف هواء السيارات

مؤيد عبد النبي محمد
باحث
قسم الهندسة الميكانيكية
كلية الهندسة – جامعة بغداد

عصام محمد علي الجبوري
استاذ مساعد
قسم الهندسة الميكانيكية
كلية الهندسة – جامعة بغداد

الخلاصة

في هذا البحث تم اجراء تحليل عملي لنوعين من المكثفات هما المكثف التقليدي ذو الانبوب الدائري والمكثف المايكروي في دورة تثليج انضغاطية خاصة بالسيارة تعمل بمائع R134a وتم اجراء التحليل بالنسبة للطاقة ومعامل انتقال الحرارة. تم اختبار اداء المكثفين والدورتين بالنسبة لتغير درجات الحرارة المحيطة بحيث تم تغييرها من 40 الى 65 درجة مئوية بينما تم تثبيت درجة حرارة المقصورة الداخلية للسيارة عند 23 درجة مئوية وكذلك حمل التبريد الداخلي 2200 واط. أظهرت النتائج المستحصلة ان المكثف المايكروي يمتلك معامل انتقال حرارة على جهة مائع التثليج وعلى جهة الهواء اعلى بـ 224% و 77 % مقارنة مع المكثف التقليدي. ولذلك، فقد وُجد ان معامل اداء الدورة الانضغاطية ذات المكثف المايكروي اعلى بـ 20 % من تلك التي تحتوي على المكثف التقليدي. اضافة الى ذلك، فان حجم المكثف المايكروي اصغر بـ 50 % من المكثف التقليدي. لذلك فإن استخدام المكثف المايكروي يوفر مساحة شاغرة اكبرفي السيارة ليتم استخدامها للاجزاء الاخرى من المحرك.

الكلمات الرئيسية: تكييف السيارة، المكثف، قنوات مايكروية، معامل انتقال الحرارة، الطاقة.

1. INTRODUCTION

One of the basic problems in the refrigeration cycle, specifically the one containing an air-cooled condenser, is the high condensing temperature. The condensing temperature may rise because of the increased temperature of the environment, especially in hot countries like Iraq. In fact, the vapor compression refrigeration cycle (VCRC) will suffer from a reduction in performance when the ambient temperature increases. Because, with rising temperature, the compressor discharge pressure increases due to the reduction in heat sink ability in receiving heat. The increased discharge pressure results in high compressor work, low refrigeration effect, and thus low coefficient of performance. Now, a new solution may be the key to design a very effective condenser, even at high ambient temperature, is by using a new type of a very compact heat exchanger. Alternatively, what is commonly known as the microchannels heat exchangers.

According to **Kandlikar and Grande, 2002**, the microchannels are the channels with hydraulic diameter from 10 μm to 200 μm. Also, **Mehendale, et al., 2000,** define it to be from 1μm to 100 μm hydraulic diameter. Another study by **Satish, et al., 2006,** considered the fluid flow behavior inside the microchannel to construct the definition. Moreover, the microchannel condenser usually designed with a multi-louvered fin and multiport, parallel tube arrangement. On the other hand, the microchannels have an increased application as future alternatives for the traditional heat exchangers and also in the medical applications, **Ohadi, et al., 2013**.

Many studies are made to investigate the heat transfer throughout the microchannel condenser and its effects on the refrigeration cycle, such as **Park and Hrnjak, 2008,** who carried out a comparison in performance between a traditional and a prototype microchannel condensers. The experiments take place in a residential air conditioning system with refrigerant R410A. The two condensers manufactured in the same face area, external volume, and fin density. However, the traditional condenser is round tube with 9.5 mm outside diameter while the microchannel condenser is rectangular with 1.9×21 mm tube cross-sectional area. The results showed that using a microchannel condenser leads to improve the cycle performance as well as a condenser and evaporate capacities for the same operating conditions. Also, they found that the use of a microchannel condenser leads to a 9 % reduction in refrigerant charge. **Shah, 2010,** investigated the condensation inside mini/microchannels by the use of his well-verified correlation, **Shah, 2009**. The correlation was shown to have 500 correct predictions with 15.9 mean error from the experiments over variance functional parameters which were: the reduced pressure varied from 0.048 to 0.52, the hydraulic diameter from 0.49 mm to 5.3 mm and the mass fluxes from 50 to 1400 kg/m^2 s for 8 different fluid condensates inside rectangular and round tubes for both the single port and multiport channels. Finally, the correlation was found to be in good agreement with 15 studies for round and multiport tubes and with a hydraulic diameter from 0.49 mm to 5.3 mm.

Wang and Rose, 2008, presented a theoretical model for condensation inside microchannels. The model takes into consideration the gravity effect, the shear stress on the surface of the condensate fluid, the pressure gradient caused by the surface tension and the effect of channel inclination. The analysis was carried out for different channel shapes, dimensions, vapor mass velocity and various temperature differences between the surface and the vapor. They found that the vapor local parameters cannot be measured directly without uncertainties in values. However, it can be measured with less inaccuracy by calculating the parameters at the inlet and the outlet of the microchannel. Also, they found that for all fluids, mass fluxes and channel configurations,

the heat flux for the same temperature difference between the vapor and the surface is constant. That means the heat flux is independent of the channel area and the fluid mass flow rate.

Kim and Mudawar, 2012, examined the heat transfer coefficient and the pressure drop characteristics for condensation inside the rectangular microchannel. A theoretical control volume has presented for FC-72 based on the smooth interface between the vapor region and the annular liquid film which is assumed to be uniform all over the perimeter of the microchannel. Experimental work was carried out to test the validity of the theoretical model. Moreover, this work done with a 24 individual experiment included various mass fluxes and four distinctive water flow rates used to cool the condenser. The model was compared with other data points of other studies, and it shows a good convergence with almost all of them. **Kim and Mudawar, 2013,** developed two general correlations for condensation heat transfer coefficient inside mini/microchannel for different substances, properties, geometries, and flow parameters. They found their new correlations by fitting large database curves. This database consists of 1964 data for single channel and 2081data for multi-channel, while the ranges of the tested parameters were; 0.424-6.22 mm hydraulic diameter and 53-1403 kg/m^{2}s mass flux for only for smooth surfaces. Furthermore, these two new correlations proposed for annular, slug and bubbly flows, and they showed good predictions with an overall error of 16 %.

AL-Hajri, et al., 2013, carried out an experimental examination for condensation inside microchannels to explore the effect of mass flux, saturation temperature and inlet degree of superheat on the heat transfer coefficient and pressure drop characteristics in a rectangular microchannel condenser. The microchannel condenser has 0.4×2.88 mm a cross-section area, 190 mm long, 7:1 aspect ratio, 0.7 mm hydraulic diameter, 6.4 mm wetted perimeter and 2 mm thickness. The experiments have been executed for two refrigerants; R134a and R245fa. The domains of the tested parameters which were; 50-500 kg/m^{2}s mass flux, 30-70°C saturation temperature, 0-15°C degree of inlet superheat and 7-115 W cooling load. The results showed that the heat transfer coefficient and the pressure drop are powerful functions of mass flux and saturation temperature, both of them are increasing with mass flux and decreasing with saturation temperature. Also, they discovered that the inlet degree of superheat has no considerable influence on the heat transfer coefficient nor on the pressure drop.

Goss and Passos, 2013, 2015, investigated the local heat transfer coefficient and the pressure drop experimentally during the condensation of R134a inside eight multiport parallel tubes with 0.77 mm hydraulic diameter of the microchannel condenser. The factors subjected to examination were; refrigerant mass flux varied from 230 to 445 kg/m^{2}s, pressure from 7.3 to 9 bar, heat flux from 17 to 35 kW/m^2 and vapor quality from 0.55 to 1. They detected that the mass flux and the dryness fraction have the utmost influence on the heat transfer coefficient than other parameters. Besides, the resistance of heat transfer is mainly caused by the film weak conduction, especially at 0.95 dryness fraction. As for the pressure drop, they found that it has a direct and an inverse proportion of mass velocity and saturation temperature respectively. In addition, almost 95 % of losses in pressure were caused by frictions.

Huang, et al., 2014, provided an air to a refrigerant model based on the finite volume method to simulate the condensation in microchannels. The model is made for multiple tube and fin shapes in order to provide the maximum adaptive geometry which enhances the thermal performance and reduces cost. The model showed very well effectiveness for 227 data points of sever-

al experiments includes eight different working fluid as well as four various geometries. The results showed that the average rate of perversion from the measured values is only 2.7 %. Also by finite volume method, **Yin, et al., 2015,** developed a numerical model for condensation inside microchannels. Their model includes one and two slabs microchannel condenser and it covers some factors of significant impact on the condenser, which are; the non-uniform air temperature, the refrigerant maldistribution through the tubes, the face velocity, and the fin conductivity. The outcomes illustrated that the asymmetric airflow affects the performance of condenser by 1.5 % for heat transfer, 6.8 % for pressure drop and 12.5 % for a refrigerant charge in the one slab microchannel condenser. While for the two slobs it is affecting the performance overall by 0.5 % for overall capacity and 9.7 % for the pressure drop in the refrigerant side. Also, they found that the fin conductivity in the transverse section partially effects by 0.06 % for overall capacity and 0.16 % for pressure drop.

The objective of the present study is to compare experimentally the performance of air-cooled finned tube and microchannel condensers in an automotive vapor compression refrigeration cycle in hot and dry climate conditions. The performance of two condensers and cycles tested under different outside ambient temperature which it was varied from 40°C to 65°C with step $\Delta T = 5$°C. Both condensers performance with respect to heat transfer coefficient and energy used R134a as the working fluid.

2. EXPERIMENTAL FACILITIES AND CONDENSERS DESCRIPTION

The test facility is shown in **Fig.1**. It consists of the test rig, the test room, and the measuring equipment. The test rig is an automobile air conditioner training unit operating with refrigerant R134a. It includes the complete car air conditioner fitted on a wheeled steel frame together with the driving motor. The unit is composed of the following components: multicylinder compressor with electromagnetic clutch, forced air condenser, an evaporator with multispeed fan, liquid receiver, and filter drier, thermostatic expansion valve, pressure switch, and turbine flow meter. A schematic diagram of the test rig is shown in **Fig.2**, while **Table 1** provides general specifications of it. Moreover, the test rig is a simulation of the car air conditioning system. So that, the device is consisting of two separate compartments: the passengers' compartment and the environment compartment. The passengers' compartment is insulated from the surrounding and from the environment compartment by a glass layer to represent the car glass windows. The passenger's compartment contains the evaporator, an electrical heater to simulate the load inside the compartment and the thermostatic expansion valve, while environment compartment contains the compressor, the electrical motor, the condenser, and the filter drier.

Fig.3 shows a photograph of the two condensers while **Table 2** and **3** provide the technical data of the microchannel and conventional round tube condensers respectively. Due to limitations in manufacturing, the microchannel condenser has different areas from the baseline round tube condenser as illustrated in **Table 4**. The condenser (the round tube condenser or the microchannel) is, fitted to the main frame by screw connections and is supplied with an axial fan that works with the cycle to increase the air flow rate when the condensation temperature rises. The condenser fan controlled by the pressure switch that it starts at 15 bar and stops at 12 bar.

The test room that already shown in **Fig.1** has used to simulate the outdoor temperature of automotive. Because it enables temperature control inside it to create a variable range of outdoor

temperatures that exist it the real car. Finally, it should be noted that the ranges of the measured parameters are given in **Table 5**.

3. HEAT TRANSFER ANALYSIS

During the analysis, the following assumptions were adopted:

1. Steady state

2. Constant mass flow rate throughout all parts.

3. All the condenser external area considered as a finned surface because $A_f \gg A_{un\text{-}f}$.

4. The conduction and fouling resistances are very low that can neglect.

The Engineering Equation Solver (EES) program is used to solve the mathematical model, which can be presented as follows; Firstly, the air side heat transfer coefficient can be found, experimentally, by equating the air side heat gain with the heat that transferred by convection. However, initially, the air properties must be calculated at an average air temperature given by **Nellis and Klein, 2009**:

$$T_{av,a} = \frac{T_{R,i} + T_{a,i}}{2} \tag{1}$$

Where $T_{av,a}$ is the average air temperature in (K), $T_{R,i}$ is the refrigerant temperature at the condenser inlet in (K) and $T_{a,i}$ is the air inlet temperature in (K).

The air mass flow rate is given by **Holman, 2010**:

$$\dot{m}_a = \rho_a \times V_a \times A_c \tag{2}$$

Where $\dot{m}_a$ is the air mass flow rate in (kg/s), ρ_a is the air density in (kg/m^3) and V_a is the air velocity in (m/s).

The rate heat transfer to air due to temperature rise is given by **Holman, 2010**:

$$Q_a = \dot{m}_a \times c_{p_a} \times (T_{a,o} - T_{a,i}) \tag{3}$$

Where Q_a is the heat transferred to the air in (W), c_{p_a} is the air specific heat in (J/kg.K) and $T_{a,i}$ and $T_{a,o}$ are the inlet and the outlet temperatures respectively, in (K).

Now, by using assumption (3), the amount of heat transfer to air due to convection on the outer surface is given by **Cengel, 2008**:

$$Q_a = h_a \times A_o \times \eta_o (T_w - T_{a,i}) \tag{4}$$

Where h_a is the air side heat transfer coefficient in (W/m^2.K), T_w is the average tube wall temperature in (K) and η_o is the overall surface efficiency and it was given by **Nellis and Klein, 2009**

$$\eta_o = 1 - \frac{A_f}{A_o}(1 - \eta_f) \tag{5}$$

Where A_f is the fin area in (m^2), A_o is the outer convection area in (m^2) and η_f is the fin efficiency, which can found by unitizing the EES built-in functions (Fin Efficiency functions). The An-

nular Rectangular Fin procedure of the EES program used. This procedure requires the value of the equivalent effective fin radius, which it has given by **Nellis and Klein, 2009**

$$r_{f,eff} = \sqrt{\left(A_f * \frac{p_f}{2\pi L_t} + \left(\frac{D_o}{2}\right)^2\right)} \qquad (6)$$

Where $r_{f,eff}$ is the effective fin radius in (m), p_f is the fin pitch in (m), L_t is the tube length in (m) and D_o the outside diameter of condenser tube in (m).

The evaluation of the fin efficiency in EES requires the air side heat transfer coefficient value. However, this value cannot determine without equation 4. Thus, a trial and error method of the solution must execute. So, the iteration starts with a guess value of air side heat transfer coefficient. The guess value and the effective fin radius obtained by equation 6, are used to calculate the fin efficiency by the EES built-in functions. After that, the fin efficiency is substituted into equation 5 to determine the overall surface efficiency. After that, the guess value and the overall surface efficiency are substituted in equation 4 to find the heat transfer rate. Lastly, the guess value was updated until equation 4 becomes equal to equation 3. In fact, the equivalence of the two equations gives the true value of the air side heat transfer coefficient. After calculating it, the air side resistance to heat transfer given by **Nellis and Klein, 2009**

$$R_a = \frac{1}{h_a A_o \eta_o} \qquad (7)$$

Where: R_a is the air side resistance in (K/W).

The refrigerant side heat transfer coefficient can be determined as average for the total condenser length regardless of the condenser zones. Such determination starts by estimating the total heat transfer resistance, which can write as **Holman, 2010**:

$$R_{total} = \frac{T_{R,s} - T_{a,i}}{Q_H} \qquad (8)$$

Where R_{total} is the total resistance in (K/W) and $T_{R,s}$ is the condensing temperature in (K).
By using assumption (4), the total resistance is a sum of refrigerant and air sides resistances, and it can write as **Nellis and Klein, 2009**

$$R_{total} = R_R + R_a \qquad (9)$$

Where R_R is the refrigerant side resistance in (K/W), **Holman, 2010**

$$R_R = \frac{1}{h_R A_i} \qquad (10)$$

Where: h_R is the refrigerant side heat transfer coefficient in (W/m^{2}K).

Substituting equation 10 into 9 and rearranging to obtain a direct expression of the refrigerant side heat transfer coefficient:

$$h_R = \frac{1}{A_i} \times \frac{1}{R_{total} - R_a} \qquad (11)$$

4. HEAT TRANSFER ANALYSIS OF THE MICROCHANNEL CONDENSER

The analysis of heat transfer of the microchannel condenser is the same as that in the conventional one. Because, the theory of fluid flow inside the microchannel is not considered, only the temperatures and areas are taken into account. However, the areas calculations of the microchannel condenser are quite different from the conventional since the tube arrangement and fins configuration are different. In this study, the areas calculations of the microchannel condenser are not computed because they were supplied by the manufacturing company. Finally, it must be

noted that the calculations methodology of heat transfer coefficient of each section as well as sections lengths of the microchannel condenser is not considered. The reason of not calculating such parameters is the parallel tubes arrangement that the microchannel condenser has, which requires the refrigerant mass flow rate of each passage, and the last is unknown due to an insufficient information about the internal geometry of the pipes inside the main tube.

5. MICROSCALE CONDENSATIONS PREDICTIONS METHODS

Although the correlations dealing with microscale condensation aren't a few, only two of them are found to be the closest to experiments. The properties are found at an average temperature given by equation (3.45).

Shah, 2010, presented a validation of his correlation to work at the microscale condensation processes. The new shah correlation (for horizontal tubes) assumes two flow regimes. The first regime occurs when

$$J_g \geq 0.98(Z + 0.263)^{-0.62} \tag{12}$$

Where J_g is the dimensionless vapor velocity, given by

$$J_g = \frac{x\, G_R}{\left(g\, D_i \rho_g (\rho_L - \rho_g)\right)^{0.5}} \tag{13}$$

Where g is the acceleration of gravity in (m/s^2).

Z is Shah correlating parameter, given by

$$Z = \left(\frac{1}{x} - 1\right)^{0.8} P_r^{0.4} \tag{14}$$

The new correlation uses the following two equations

$$h_I = h_{LT} \left(\frac{\mu_L}{14\mu_g}\right)^n \left((1 - x)^{0.8} + \frac{3.8 x^{0.76}(1 - x)^{0.04}}{P_r^{0.38}}\right) \tag{15}$$

Where h_I is the first regime heat transfer coefficient (W/m^{2}K), h_{LT} is the heat transfer coefficient assuming the flow is totally liquid, given by

$$h_{LT} = \frac{K_L}{D_h} * 0.023\, Re_L^{0.8}\, Pr_L^{0.4} \tag{16}$$

And

$$n = 0.0058 + 0.557\, P_r \tag{17}$$

The second equation is given by

$$h_{Nu} = 1.32\, Re_{LS}^{\frac{-1}{3}} \left(\frac{\rho_L(\rho_L - \rho_g)\, g\, K_L^3}{\mu_L^2}\right)^{\frac{1}{3}} \tag{18}$$

Where h_{Nu} is the heat transfer correlation given by Nusselt relation and K_L is the liquid refrigerant thermal conductivity in (W/m.K).

Now, for the first regime, the local condensation heat transfer coefficient is

$$h_x = h_I \tag{19}$$

For the second regime

$$h_x = h_I + h_{Nu} \tag{20}$$

Where Re_g is the gas Reynolds number, given by:

$$Re_g = \frac{G_R D_i}{\mu_g} \tag{21}$$

Shah recommended equation (3.106) for $Re_g > 35,000$ [28].

Kim and Mudawar, 2010, presented two correlations of the condensation heat transfer coefficient inside mini/micro-channel. The procedure of them is as follows:

$$X = \sqrt{\left(\frac{dp}{dz}\right)_L \Big/ \left(\frac{dp}{dz}\right)_g} \tag{22}$$

Where X is the general Lockhart- Martinelli parameter, $\left(\frac{dp}{dz}\right)_L$ and $\left(\frac{dp}{dz}\right)_g$ are the pressure gradient for the liquid and the gas respectively, and they are given by

$$-\left(\frac{dp}{dz}\right)_L = \frac{2\, f_L\, v_L\, G^2\, (1-x)^2}{D_h} \tag{23}$$

And

$$-\left(\frac{dp}{dz}\right)_g = \frac{2\, f_g\, v_g\, G^2\, x^2}{D_h} \tag{24}$$

Where v_L and v_g are the kinematic viscosity of the liquid and the gas phase respectively. And f_L and f_g are the Fanning friction factor of the liquid and the gas phase respectively, and they are given by

$$\begin{aligned}
f_{L,g} &= 16\, Re_{Ls,gs}^{-1} \quad for\ Re_{Ls,gs} < 2000 \\
f_{L,g} &= 0.079\, Re_{Ls,gs}^{-0.25} \ \ for\ \ 2000 \le Re_{Ls,gs} < 20{,}000 \\
f_{L,g} &= 0.046\, Re_{Ls,gs}^{-0.2} \ \ for\ Re_{Ls,gs} \ge 20{,}000
\end{aligned} \tag{25}$$

Where the subscript (L,g) means liquid or gas, and the (Ls,gs) means superficial liquid or superficial gas. While the superficial liquid Reynolds number is given by equation (3.96), the superficial gas is given by

$$Re_{gs} = \frac{G\, x\, D_h}{\mu_g} \tag{26}$$

The two-phase pressure drop multiplier based on gas phase ($\phi_g{}^2$) is given by

$$\varnothing_g^2 = 1 + CX + X^2 \tag{27}$$

Where C is a coefficient in Lockhart-Martinelli parameter, and it is given by

$$
\begin{aligned}
C &= 0.39\, Re_L^{0.03}\, Su_g^{0.1} \left(\frac{\rho_L}{\rho_g}\right)^{0.35} \quad for\ Re_L \ge 2000, Re_g \ge 2000 \\[2mm]
C &= 8.7x10^{-4} Re_L^{0.17} Su_g^{0.5} \left(\frac{\rho_L}{\rho_g}\right)^{0.14} \quad for\ Re_L \ge 2000, Re_g < 2000 \\[2mm]
C &= 0.0015\, Re_L^{0.59}\, Su_g^{0.19} \left(\frac{\rho_L}{\rho_g}\right)^{0.36} \quad for\ Re_L < 2000, Re_g \ge 2000 \\[2mm]
C &= 3.5x10^{-5}\, Re_L^{0.44}\, Su_g^{0.5} \left(\frac{\rho_L}{\rho_g}\right)^{0.48} \quad for\ Re_L < 2000, Re_g < 2000
\end{aligned} \tag{28}
$$

Where Su_g is the gas Suratman number, and it is given by

$$Su_g = \frac{\rho_g\, \sigma\, D_h}{\mu_g^2} \tag{29}$$

Where σ is the surface tension?

Now, after calculating ϕ_g , the local heat transfer coefficient for (smooth-annular, wavy-annular, transition) which happen at $We^* > 7X_{tt}^{0.2}$ is given by

$$h = \frac{K_L}{D_h} * 0.048 \, Re_{LS}^{0.69} Pr_{LS}^{0.34} * \frac{\emptyset_g}{X_{tt}}, \tag{30}$$

And for slug and bubbly flows where $We^* < 7X_{tt}^{0.2}$ is given by

$$h = \frac{K_L}{D_h} * \left[\left(0.048 \, Re_{LS}^{0.69} Pr_{LS}^{0.34} * \frac{\emptyset_g}{X_{tt}} \right)^2 \right.$$
$$\left. + \left(3.2x10^{-7} Re_{LS}^{-0.38} \, Su_g^{1.39} \right)^2 \right]^{0.5} \tag{31}$$

Where We^* is the modified Weber number, which is given by

$$We^* = 2.45 \frac{Re_{gs}^{0.64}}{Su_g^{0.3}(1 + 1.09X_{tt}^{0.039})^{0.4}}$$
$$We^* = 0.85 \frac{Re_{gs}^{0.79}X_{tt}^{0.157}}{Su_g^{0.3}(1 + 1.09X_{tt}^{0.039})^{0.4}} \left[\left(\frac{\mu_g}{\mu_L} \right)^2 \left(\frac{\nu_g}{\nu_L} \right) \right]^{0.084} \tag{32}$$

Where the first equation is for $Re_{Ls} \leq 1250$ while the second is for $Re_{Ls} > 1250$.

6. RESULTS AND DISCUSSION

Fig.4 shows that the refrigerant side heat transfer coefficient of the microchannel condenser is about 224 % higher than the conventional baseline condenser. The higher mass flux can explain this increment that the microchannel condenser needs. The higher mass flux resulted primarily from, the smaller flow area that caused by the very small hydraulic diameter of the microchannel condenser (0.1 mm). In fact, the microchannel condenser works with 787 kg/m²s mass flux, while the conventional baseline condenser works with 200 kg/m²s. Therefore, it has 294 % higher mass flux than the conventional condenser. So, since the refrigerant side heat transfer coefficient has a direct proportion with the mass flux, it will be higher throughout the microchannel condenser than the conventional.

However, it must be noted that, although the microchannel condenser has a 224 % larger heat transfer coefficient than the conventional, the difference in heat rejection is only 5 % as shown in **Fig.5**. However, this ratio is because the convection area has a direct proportion with heat transfer rate. Thus, the smaller the area, the smaller the heat transfer rate. In fact, the conventional round tube condenser has 0.2156 m² internal convection area, while the microchannel has 0.08 m². So that, it has a 170 % larger internal convection area than the microchannel. Therefore, the increment in heat transfer coefficient, in case of using microchannel condenser, is accompanied by a decrement in the convection area. That, if the heat transfer coefficient increased by half, for example, and the convection area decreased by half, they will cancel each other out and the same rate of heat transfer will be obtained for the same temperature difference. This fact can be seen by the ratio of (hA) product, which is

$$\frac{(hA)_{Microcahnnel}}{(hA)_{conventional}} = \frac{4174 \times 0.08}{1318 \times 0.2156} = 1.17 \tag{33}$$

Where: 4174 and 1318 W/m²K are the average refrigerant-side heat transfer coefficients of the microchannel condenser and the conventional respectively. Consequently, the increment in heat

rejection should be 17 %, not 5 % if the temperature difference assumed to be the same in both condensers. However, due to a limitation of the measuring system, the difference in temperature between the fluid and the internal wall is not measured. Also, the microchannel condenser is made from aluminum, while the conventional made from copper. So, the microchannel condenser has 20 % lower thermal conductivity than the conventional. Thus, since the thermal conductivity is different, the same temperature difference is not expected to occur. Moreover, the missing 12 % of heat rejection may be due to the prospective lower temperature difference that the microchannel condenser works with. Nonetheless, this 12 % could be due to the behave of heat transfer rate and coefficient with ambient temperature. Because, refrigerant side heat transfer coefficient and even the air side, are practical functions, which depend on large of parameters contribute together to produce the heat transfer coefficient. In fact, these parameters are not increasing or decreasing gradually or simultaneously. But, instead of that, they change in different ranges resulted, sometimes, in a nonlinear behavior of heat transfer coefficient. So, although this case did not exactly happen, it may give some justifications for points that out of the expected curve behavior which may cause some fluctuations in the difference ratio of heat transfer coefficient between the two condensers.

Fig.6 displays that the air side heat transfer coefficient of the microchannel condenser is about 77 % larger than the conventional. This ratio is due to the difference in fin configuration since the conventional condenser fins are wavy, while the microchannel fins are multi-louver. Therefore, this higher air side heat transfer coefficient of the microchannel condenser resulted in the air side heat gain to be 11 % higher than the conventional as shown in **Fig.7**. Again, it seems that the ratio of air side heat gain increment is so small compared with that of the heat transfer coefficient. However, this ratio is caused by the smaller external convection area of the microchannel condenser and the fewer temperature difference as well. In fact, the microchannel condenser has 7.14 m^2 external convection area, while the conventional condenser has 8.942 m^2. That means a 20 % reduction in the external area. Moreover, the average temperature difference between the wall and the inlet air is found to be 14.5°C and 18.5°C for the microchannel condenser and the conventional respectively. Thus, the temperature difference is reduced by 22 %. Now, by substituting these numbers into the equation of heat transfer ratio, it was found:

$$\frac{Q_{Microchannel}}{Q_{conventional}} = \frac{hA\Delta T}{hA\Delta T} = \frac{48}{27} \times \frac{7.14}{8.942} \times \frac{14.5}{18.5} = 1.11 \tag{34}$$

Where: 48 and 27 W/m^{2}K are the average air side heat transfer coefficients of the microchannel condenser and the conventional respectively. Once more, the increment in air side heat transfer coefficient accompanied with a decrement in external convection are to produce only 11 % addition to air side heat gain.

The attention should be paid for the case of exactly identical condensers. Because, as already mentioned, the microchannel condenser has different internal and external convection area than the conventional baseline condenser due to restrictions in the manufacturing process. But, if the microchannel condenser areas are exactly the same as the conventional, the heat transfer surely will be higher. Nonetheless, since the areas are different, the microchannel condenser has 50 % smaller volume than the conventional. Therefore, using the microchannel condenser can give an advantage by reducing the material used in manufacturing as well as the space requirement for installation because it has smaller size and higher thermal performance than the conventional condenser.

Fig.8 shows that the microchannel condenser cycle has 9 % lower discharge pressure than the conventional one because of the higher heat rejection in the microchannel condenser. However, the discharge pressure, whenever it rises, resulting in significant impacts on the refrigeration cycle. The most two significant effects are the higher compressor work that is needed to accomplish the compression, and the lower refrigeration effect. Because of the higher work needed since the difference between inlet and outlet entropies will be higher. In another word, the compressor should spend more power to compress the hot gas. Because of this hot gas will have a higher resistance to compression each time with rising ambient temperature due to the higher internal energy inside it. Therefore, more work is required to complete it. Regarding the lower refrigeration effect, it happens because the enthalpy that leaves the condenser increase with saturation temperature or pressure. So, the refrigeration effect will be lower since the same leaving enthalpy will enter the evaporator. Finally, because the COP is the ratio of refrigeration effect to specific compressor work, it will decrease with the higher pressure, or, in a different expression, the higher ambient temperature.

Now, due to all the above, and, since the microchannel cycle works with lower discharge pressure, it has about 20 % higher COP than the typical cycle, as shown in **Fig.9**. Also, the lower discharge pressure in it leads to 10 % lower compressor work as shown in **Fig.10**, and 7 % higher refrigeration effect as shown in **Fig.11**.

Fig.12 shows a P-h diagram of the conventional and the microchannel cycle. It seems that at 40ºC ambient temperature and 8.5 m/s airspeed, the discharge pressures are 18 bar and 15 bar for the conventional and the microchannel cycle respectively. Also, at 60ºC and 8.5, the pressures are 24 bar and 23 bar respectively. So that, the microchannel cycle has about 9 % lower discharge pressure than the conventional. It is obvious that the microchannel cycle works with lower discharge pressure because it has higher heat rejection and saturation temperature as mentioned before. So that, it will have better performance than the conventional cycle as it will be explained in detail. However, it must be noted that the microchannel condenser has a higher pressure drop than the conventional. This pressure drop is well presented on by the inclined line of the microchannel cycle. This drop in pressure is happing due to the high flow resistance which caused by the small passages of the microchannel condenser. Besides, the pressure drop was found to be increasing with ambient temperature and decreasing with condenser airspeed. That at 40, 50 and 60ºC ambient temperature, the pressure drop was 1, 1.5 and 2 bar as average respectively. While with 4, 6.25 and 8.5 m/s airspeed, it was 1.75, 1.3 and 1 bar as average respectively. Nonetheless, the effect of pressure drop is not considered in this study.

7. CONCLUSIONS

In this study, the conventional finned tube condenser of the automotive air conditioning cycle replaced with a microchannel condenser to test whether the microchannel condenser can improve the cycle performance, especially at the high ambient temperature. The study is carried out experimentally for both cycles (the typical cycle and the microchannel cycle). However, the heat transfer areas of the two condensers are not the same as already shown in **Table 4**. This case is due to a manufacturing limitation regarding the microchannel condenser. Now, the upcoming conclusions which were reached.

1. The microchannel condenser has 224 % and 77 % higher refrigerant side and air side heat transfer coefficients respectively than the conventional round tube condenser.

2. The heat rejection increased only by 5 % due to the reductions in internal and external convection areas by using the microchannel condenser.

3. The microchannel condenser can reduce the space required for installation and save cost since it has a 50 % smaller volume than the conventional round tube condenser.

4. The microchannel condenser cycle has 9 % lower discharge pressure, 20 % higher COP, 10 % lower work, 10 % higher heat absorption and.

ACKNOWLEDGMENTS

REFERENCES

- S. G. Kandlikar and W. J. Grande, 2002, Evolution of microchannel flow passages − Thermohydraulic performance and fabrication technology, *ASME Int. Mech. Eng. Congr. Expo.*, pp. 1–13.

- S. S. Mehendale, A. M. Jacobi, and R. K. Shah, 2000, Fluid Flow and Heat Transfer at Micro- and Meso-Scales With Application to Heat Exchanger Design, *Appl. Mech. Rev.*, vol. 53, no. 7, p. 175.

- M. R. K. Satish G. Kandlikar, Srinivas Garimella, Dongqing Li, Stéphane Colin, 2006, *Heat transfer and fluid flow in minichannels and microchannels*. ELSEVIER.

- M. Ohadi, K. Choo, S. Dessiatoun, and E. Cetegen, 2013, *Next Generation Microchannel Heat Exchangers*. Springer.

- C. Y. Park and P. Hrnjak, 2008, Experimental and numerical study on microchannel and round-tube condensers in a R410A residential air-conditioning system, *Int. J. Refrig.*, vol. 31, no. 5, pp. 822–831.

- M. M. Shah, 2010, Heat Transfer During Condensation Inside Small Channels: Applicability of General Correlation for Macrochannels, *14th Int. Heat Transf. Conf.*, no. 1, pp. 1–10.

- M. M. Shah, 2009, An Improved and Extended General Correlation for Heat Transfer During Condensation in Plain Tubes, *ASHRAE*, vol. 15, no. 5, pp. 889–914.

- H. S. Wang and J. W. Rose, 2011, Theory of heat transfer during condensation in microchannels, *Int. J. Heat Mass Transf.*, vol. 54, no. 11–12, pp. 2525–2534, May.

- S. M. Kim and I. Mudawar, 2012, Theoretical model for annular flow condensation in rectangular micro-channels, *Int. J. Heat Mass Transf.*, vol. 55, no. 4, pp. 958–970.

- S. Kim and I. Mudawar, 2013, Universal approach to predicting heat transfer coefficient for condensing mini / micro-channel flow, *Int. J. Heat Mass Transf.*, vol. 56, no. 1–2, pp. 238–250.

- E. Al-Hajri, A. H. Shooshtari, S. Dessiatoun, and M. M. Ohadi, 2013, Performance characterization of R134a and R245fa in a high aspect ratio microchannel condenser, *Int. J. Refrig.*, vol. 36, no. 2, pp. 588–600.

- G. Goss and J. C. Passos, 2013, Heat transfer during the condensation of R134a inside eight parallel microchannels, *Int. J. Heat Mass Transf.*, vol. 59, pp. 9–19, Apr.

- G. Goss, J. L. G. Oliveira, and J. C. Passos, 2015, Pressure drop during condensation of R-134a inside parallel microchannels, *Int. J. Refrig.*, vol. 56, pp. 114–125, Aug.

- L. Huang, V. Aute, and R. Radermacher, 2014, A model for air-to-refrigerant microchannel condensers with variable tube and fin geometries, *International Journal of Refrigeration*, vol. 40. pp. 269–281.

- X. Yin, W. Wang, V. Patnaik, and J. Zhou, 2015, Evaluation of microchannel condenser characteristics by numerical simulation, *Int. J. Refrig.*, vol. 54, pp. 126–141.

- G. F. Nellis and S. a. Klein, 2009, *Heat Transfer*. Cambridge University Press.

- J. Holman, *Heat Transfer*. McGraw-Hill 2010.

- Y. A. Cengel, 2008, Introduction to Thermodynamics and Heat Transfer, McGraw-Hill.

NOMENCLATURE

A	area (m^2)	ρ	Density (kg/m^3)
B	vertical distant between condenser tubes (m)		
C	horizontal distant between condenser tubes (m)	*Subscripts*	
C_p	specific heat (J/kg.K)	A	air
D	diameter (m)	Av	average
h	heat transfer coefficient (W/m^{2}K)	C	cross-sectional
H	condenser height (m)	col	condenser tubes columns
L	length (m); also condenser length in the air flow direction (m)	eff	effective
$\dot{m}$	mass flow rate (kg/s)	F	fin
N	number (-)	H	high
P	pitch (m)	I	inlet; also inner

P	pressure (Bar)
Q	heat transferred (W)
R	radius (m)
R	resistance (K/W)
T	temperature (ºC or K)
Th	thickness (m)
V	velocity (m/s)
W	work

O	outlet; also
R	refrigerant
T	tube
total	total
Un-fin	un-finned

Greek symbol

η   Efficiency

Abbreviations

COP	coefficient of Performance
EES	engineering Equation Solver
HTC	heat Transfer Coefficient
VCRC	vapor Compression Refrigeration cycle

Figure 1. Test rig
(1) Test room frame (2) Test room door (3) Thermometer display (4) Test rig (5) Vane an-
emometer display (6) Temperature Recorder (Data Logger) (7) Thermocouples (8) PC
computer (9) secondary pressure gauge (10) LapJack USB wire (11) Temperature sensors
wires (12) lapJack container
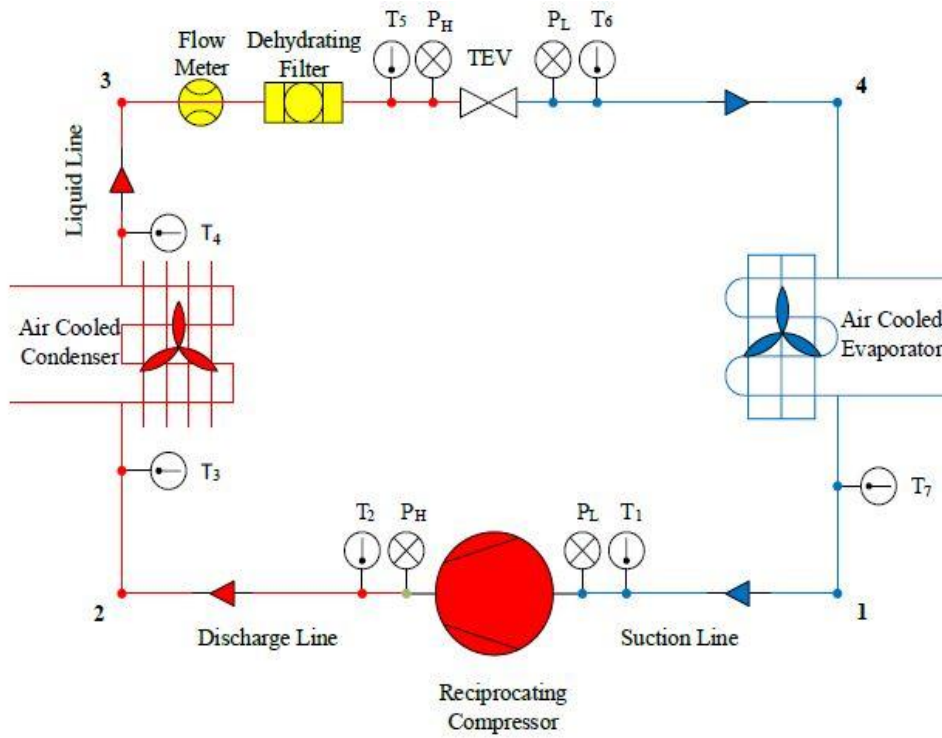
Figure 2. Schematic diagram of the test rig.

Figure 3.a. Round tube condenser   **Figure 3.b.** Microchannel condenser
Figure 3. Photograph of the two condensers.
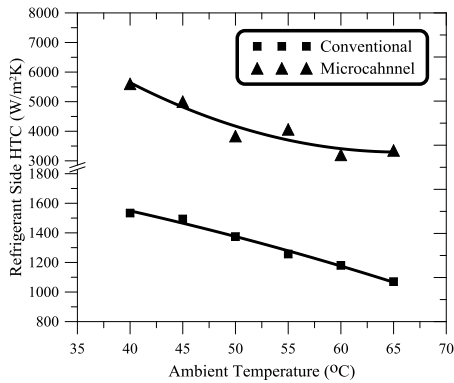
Figure 4. Refrigerant side htc vs. Ambient temperature.
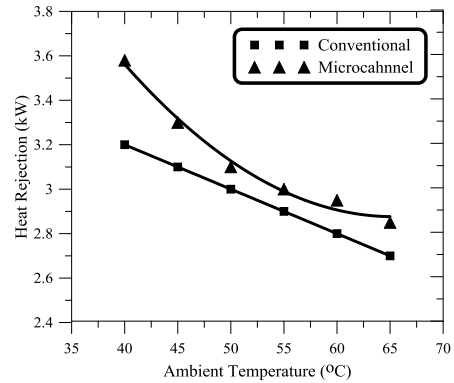
Figure 5. Heat rejection vs. Ambient temperature.
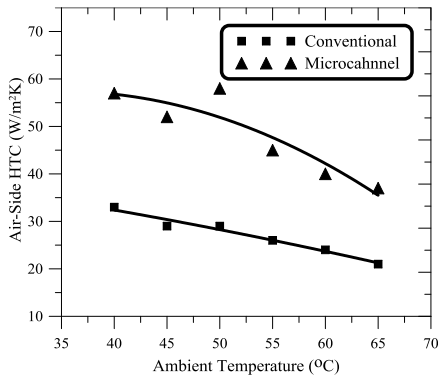
Figure 6. Air side htc vs. Ambient temperature.
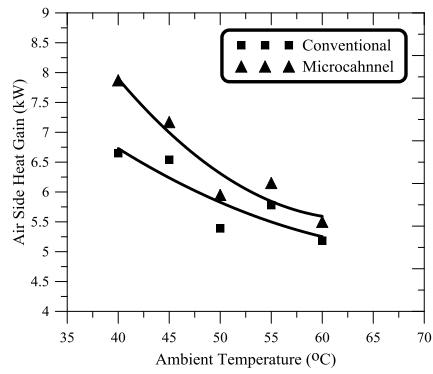
Figure 7. Air side heat gain vs. Ambient temperature.
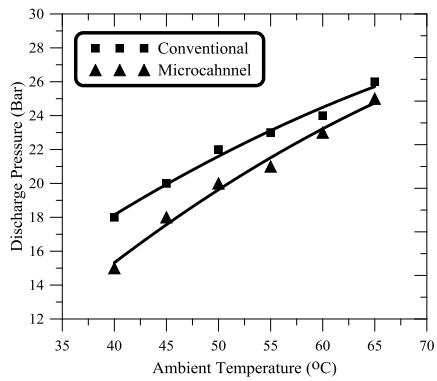
Figure 8. Discharge pressure vs. Ambient temperature.
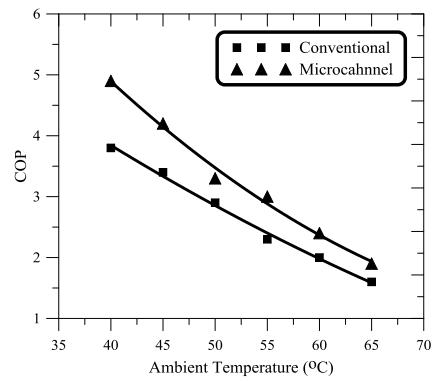
Figure 9. COP vs. Ambient temperature.
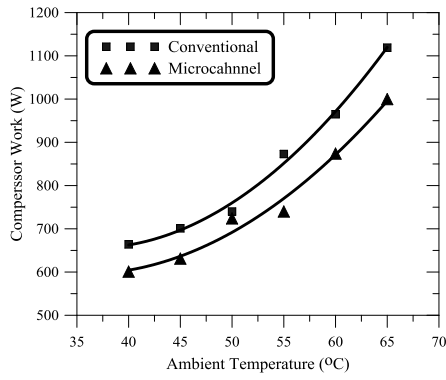
Figure 10. Compressor work vs. Ambient temperature.
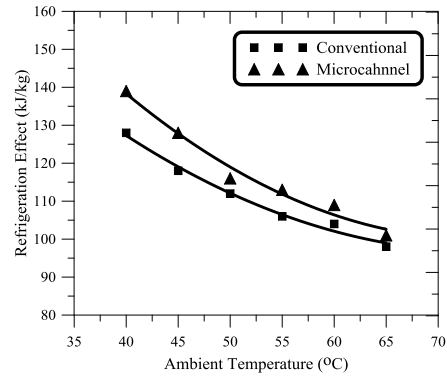
Figure 11. Refrigeration effect vs. Ambient temperature.
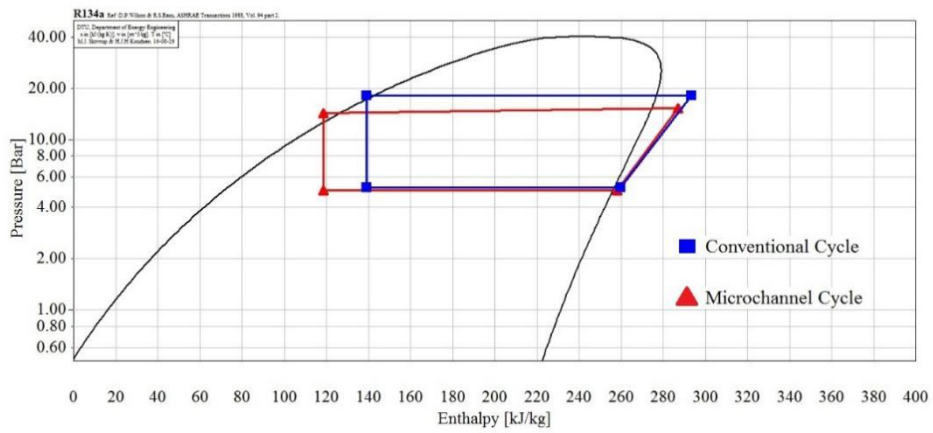
(a) At T_a= 40°C and V_a= 8.5 m/s
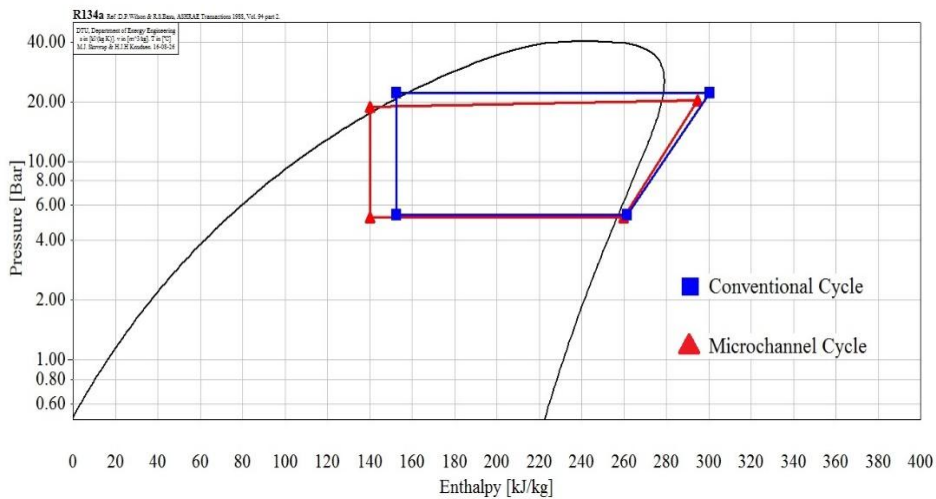
(b) At T_a= 50°C and V_a= 8.5 m/s
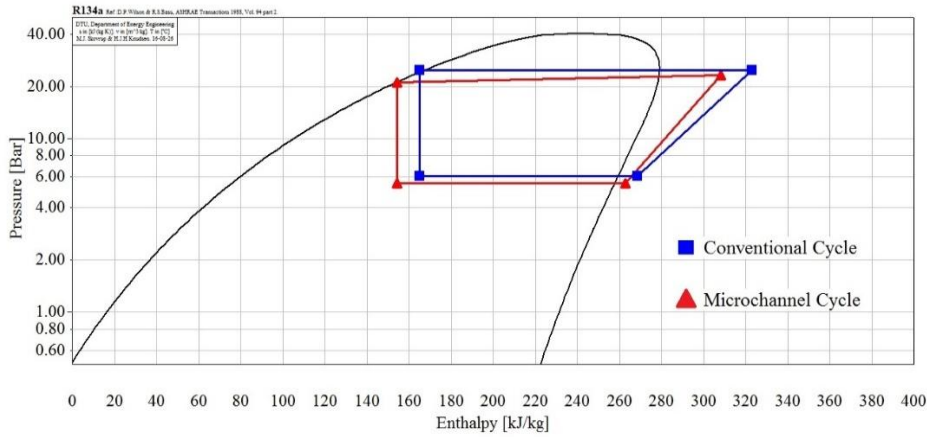
(c) At T_a= 60° C and V_a= 8.5 m/s

Figure 12. P-h Diagram of the Two Cycles.

Table 1. Test rig general specifications.

Parameter	Specifications
Manufacturer company	Product Engineering – Italy
Type	GR030/000/009D
Serial number	6331/0000/000÷6355/0000/000
Manufacturing year	2003
Net weight	84 kg
Gross weight	180 kg
Dimensions	580×610×1400 mm
Working fluid	R134a

Table 2. Microchannel condenser Specifications.

Parameters	Specification
Material	Aluminum
Tube arrangement	Parallel
Height	395 mm
Length	431 mm
Depth	25.4 mm
Hydraulic diameter	0.1 mm
Tube cross section	Rectangle
Tube thickness	0.4 mm
Fin material	Aluminum
Fin configuration	Corrugated sheets
Fin thickness	0.1 mm
Fin pitch	2.2 mm
Refrigerant	R22, R134a
Manufactured company	YiWu ShuangChuang Refrigeration Equipment Co, Ltd
Serial number	MC-2501-900

Table 3. Conventional round tube condenser specifications.

Parameters	Specifications
Height	330 mm
Width	330 mm
Length in air flow direction	90 mm
Outside diameter	10 mm
Inside diameter	8 mm
Tube wall thickness	1 mm
Fin thickness	0.08 mm
Fin pitch	2.08 mm
Vertical distant between tubes	15.7 mm
Horizontal distant between tubes	33.6 mm
Number of rows	4
Number of tubes per row	26
Number of fins	150
Fan diameter	280 mm

Table 4. Range of operational conditions.

Parameter	Range
Ambient temperature	40-65 ^{o}C, ΔT= 5 ^{o}C
Discharge pressure	14- 28 bar
Suction pressure	5-6 bar
Saturation temperature	53- 84 ^{o}C
Condenser air speeds	8.5 m/s
Indoor temperature	23 ^{o}C
Cooling load	2200 W
The cooled space dimensions	580 x 610 x 300 mm
Refrigerant mass flow rate	0.02 kg/s
Refrigerant mass flux	200 kg/m^2 s; for conventional cycle 787 kg/m^2 s; for microchannel cycle